AIP Journal of Applied Physics

Nanotwin and phase transformation in tetragonal Pb (Fe 1 / 2 Nb 1 / 2) 1 − x Ti x O 3 single crystal

C.-S. Tu, C.-T. Tseng, R. R. Chien, V. Hugo Schmidt, and C.-M. Hsieh

Citation: Journal of Applied Physics **104**, 054106 (2008); doi: 10.1063/1.2974791
View online: http://dx.doi.org/10.1063/1.2974791
View Table of Contents: http://scitation.aip.org/content/aip/journal/jap/104/5?ver=pdfcov
Published by the AIP Publishing

Nanotwin and phase transformation in tetragonal $Pb(Fe_{1/2}Nb_{1/2})_{1-x}Ti_xO_3$ single crystal

C.-S. Tu,[1,a)] C.-T. Tseng,[2] R. R. Chien,[3] V. Hugo Schmidt,[3] and C.-M. Hsieh[2]
[1]*Graduate Institute of Applied Science and Engineering, Fu Jen Catholic University, Taipei, Taiwan 242, Republic of China*
[2]*Department of Physics, Fu Jen Catholic University, Taipei, Taiwan 242, Republic of China*
[3]*Department of Physics, Montana State University, Bozeman, Montana 59717, USA*

(Received 14 March 2008; accepted 1 July 2008; published online 5 September 2008)

This work is a study of phase transformation in (001)-cut $Pb(Fe_{1/2}Nb_{1/2})_{1-x}Ti_xO_3$ (x=48%) single crystals by means of dielectric permittivity, domain structure, and *in situ* x-ray diffraction. A first-order $T(T_{NT})$-$C(T_{NT})$ phase transition was observed at the Curie temperature $T_C \cong 518$ K upon zero-field heating. T, T_{NT}, and C are tetragonal, tetragonal nanotwin, and cubic phases, respectively. $T(T_{NT})$ and $C(T_{NT})$ indicate that minor T_{NT} domains reside in the T and C matrices. Nanotwins, which can cause broad diffraction peak, remain above $T_C \cong 518$ K and give an average microscopic cubic symmetry in the polarizing microscopy. Colossal dielectric permittivity ($>10^4$) was observed above room temperature with strong frequency dispersion. This study suggests that nanotwins can play an important role in relaxor ferroelectric crystals while phase transition takes place. The Fe ion is a potential candidate as a *B*-site dopant for enhancing dielectric permittivity. © *2008 American Institute of Physics*. [DOI: 10.1063/1.2974791]

I. INTRODUCTION

Polar nanostructures are possibly the most important feature in relaxor ferroelectrics (FEs) because they are responsible for FE properties and phase transformations. Ferroelastic crystals often consist of structural twins to accommodate the spontaneous lattice distortion and minimize the elastic strain energy. A nanotwin diffraction theory was recently developed by Wang,[1,2] showing that tetragonal (T) nanotwins of {101} twin plane can mimic monoclinic M_C phase, and rhombohedral (R) nanotwins of {001} and {110} twin planes can mimic monoclinic M_A and M_B phases, respectively. Since the nanotwin (or nanodomain) size is much smaller than the coherent length of diffraction radiation, scattered waves from individual nanodomains coherently superimpose in diffraction. Thus broadening of the reflection peak is expected.[2] Tetragonal nanotwins (T_{NT}) with domain size of about 10 nm have been observed in (001)-cut PMN-33%PT crystal by transmission electron microscopy (TEM).[3]

High-strain FE $Pb(Mg_{1/3}Nb_{2/3})_{1-x}Ti_xO_3$ (PMN-PT) and $Pb(Zn_{1/3}Nb_{2/3})_{1-x}Ti_xO_3$ crystals have demonstrated their value in piezoelectric and medical ultrasonic imaging devices.[4,5] To improve thermal stability, it has been a goal to find crystals with high Curie temperature (T_C) and dielectric permittivity. Multiferroic phenomena that couple electric, magnetic, and structural order parameters have drawn much attention recently because of potential applications in information storage, spintronics, and sensors.[6,7] Among high-T_C piezoelectric crystals with potential multiferroic properties, $Pb(Fe_{1/2}Nb_{1/2})_{1-x}Ti_xO_3$ (PFN-PT) compounds have drawn interest in recent years.

The FE $Pb(Fe_{1/2}Nb_{1/2})O_3$ (PFN) ceramics were found with T_C=385 K in 1958.[8] An antiferromagnetic phase transition was proposed below 9 K in PFN crystal.[9] A R–monoclinic (M)–cubic (C) sequence transition was reported near 354 and 383 K in PFN crystal by polarizing microscopy and thermal analysis.[10] X-ray and synchrotron results suggested a M-T-C sequence transition near 355 and 376 K in PFN crystal and powders.[11] Neutron powder diffraction of PFN ceramics revealed a R phase with *R*3*m* symmetry at 10 and 300 K.[12] These contradictions between macroscopic phases could be due to the ordering degree of Fe^{3+} and Nb^{5+} ions at *B*-sites. It was proposed that *B*-site disorder tends to cause R symmetry, but 1:1 ordering of Fe^{3+} and Nb^{5+} ions would dictate a reduction of the symmetry to M phase.[12] PFN ceramics show a FE-paraelectric transition at $T_C \cong 370$ K and strong frequency-dependent dielectric permittivity, associated with the cation disorder at the *B*-site of the $A(B_I^{3+}B_{II}^{5+})O_3$ lattice.[13] Ferromagnetism was observed at room temperature in PFN powder.[13]

From x-ray diffraction (XRD) and thermal results, a phase diagram of PFN-PT ceramics was proposed with the morphotropic phase boundary in the region $0.1 \leq x \leq 0.2$.[14] A R-T-C sequence transition was proposed near 423 and 473 K in the (001)-cut PFN-6%PT crystal by TEM.[15] PFN-6%PT crystal exhibits high dielectric permittivity on the order of 10^5 for measuring frequency $f < 100$ kHz, but no Curie temperature was found below 570 K.[16] A broad dielectric dispersion was observed and was attributed to hopping conduction of 3*d* electrons between equivalent Fe ion positions.[16] Gao *et al.*[17] reported that the unpoled PFN-48%PT crystal exhibits an abnormal dielectric behavior and high dielectric loss, associated with hole conductivity by partial reduction of Fe^{3+} to Fe^{2+}.

Phase thermal stability and dynamics of nanostructure have been important issues in relaxor FE crystals. Both in

a)Author to whom correspondence should be addressed. Electronic mail: 039611@mail.fju.edu.tw.

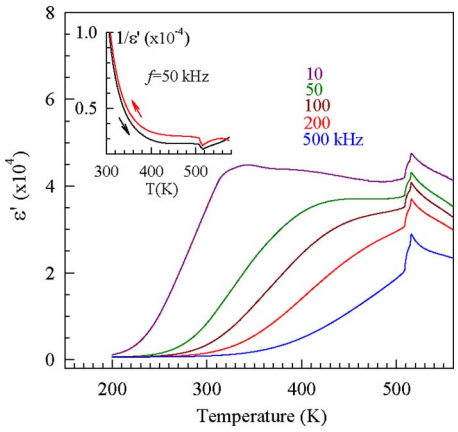

FIG. 1. (Color online) Frequency-dependent ZFH dielectric permittivity. The ZFH and ZFC $1/\varepsilon'$ were taken at $f=50$ kHz.

this crystal and in other PFN-PT crystals,[16,17] the dielectric permittivity upon zero-field heating (ZFH) shows high dielectric permittivity with strong frequency dispersion (as seen in Fig. 1). However, phase transition, microscopic structures, and their correlation have not been well understood. In this work, we have investigated temperature-dependent phase transformation in the (001)-cut PFN-48%PT crystal by means of dielectric permittivity, domain observation, and *in situ* XRD. It was found that tetragonal nanotwins play an essential role during the phase transition.

II. EXPERIMENTAL PROCEDURE

The PFN-48%PT (starting composition) single crystal was grown using a modified Bridgman method. For dielectric measurements, a Wayne Kerr analyzer PMA3260A was used to obtain the real part ε' of dielectric permittivity. The sample was cut perpendicular to the ⟨001⟩ direction with dimensions of $4.0\times5.8\times0.7$ mm^3. The basal surfaces of sample were deposited with gold electrodes. Two processes were used in the dielectric measurements and are called "zero-field heating" and "zero-field cooling" (ZFC), in which the data were taken upon heating and cooling without any poling, respectively. A Janis CCS-450 cold head was used with a Lakeshore 340 temperature controller with heating/cooling rate of 1.5 K/min.

Domain structures were observed by using a Nikon E600POL polarizing microscope with a crossed polarizer/analyzer (P/A) pair. The sample thickness was about 70 μm. Angles of the P/A pair in this work were measured with respect to the [110] direction. The experimental setup and details for using optical extinction to determine domain phase can be found in Ref. 18.

A high-temperature Rigaku model Multiflex x-ray diffractometer with Cu $K\alpha_1$ ($\lambda=0.154\,06$ nm) and Cu $K\alpha_2$ ($\lambda=0.154\,44$ nm) radiations was used for *in situ* symmetry study of unit cell. The intensity ratio between $K\alpha_1$ and $K\alpha_2$ radiations is about 2:1.[19] To avoid surface stress caused by polishing, the sample was annealed at 623 K ($>T_C\cong518$ K) for about 30 min before XRD scans. The sample thickness was 0.70 mm and the x-ray penetration depth was less than 10 μm.[20] The 2θ-XRD spectra were fitted by using PEAKFIT software with the sum of Gaussian and Lorentzian terms. The $K\alpha_1$ and $K\alpha_2$ peaks for the same reflection should have essentially the same separation and ratio of full width at half maximum.

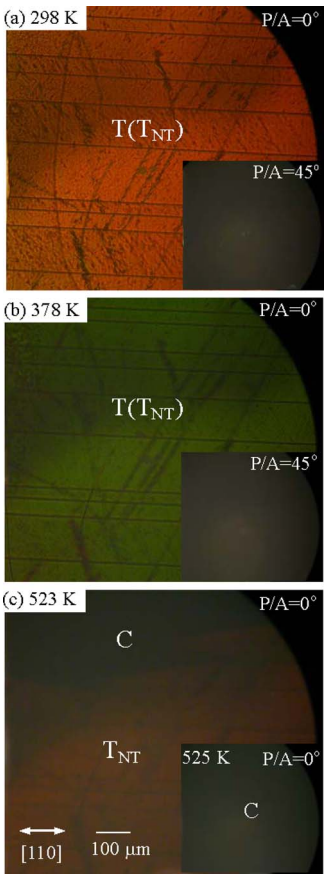

FIG. 2. (Color online) Domain structures taken at P/A=0° and 45° upon ZFH. T, T_{NT}, and C are tetragonal, tetragonal nanotwin, and cubic phases, respectively.

III. RESULTS AND DISCUSSION

Figure 1 gives the temperature- and frequency-dependent dielectric permittivity ε' upon ZFH. ε' varies from 1×10^2 to 4.5×10^4 near room temperature and exhibits strong frequency dispersion. The broad frequency-dependent plateau (or shoulder) shifts toward higher temperature with increasing frequency. This feature is possibly associated with the relaxation of mobile charge carrier due to hole conductivity by partial reduction of Fe^{3+} to Fe^{2+}.[17] ε' and $1/\varepsilon'$ (inset of Fig. 1) show a clear frequency-independent maximum peak at $T_m\cong515$ K and a wide-range thermal hysteresis in the region of ~300–515 K, implying a first-order phase transition.

Figure 2 illustrates the temperature-dependent domain structures observed at P/A=0° and P/A=45° for 298, 378, 523, and 525 K upon ZFH. Below 523 K, the whole domain matrix exhibits extinction angle at P/A=45° associated with 90°-domain walls (or [110] oriented striations), indicating that a major T phase mixed with T-phase nanotwins (which can mimic M_C phase in the T matrix with the same extinction at P/A=45°).[18] The 90°-domain walls in Fig. 2 resemble those seen from [100] and [010] T microdomains and/or nan-

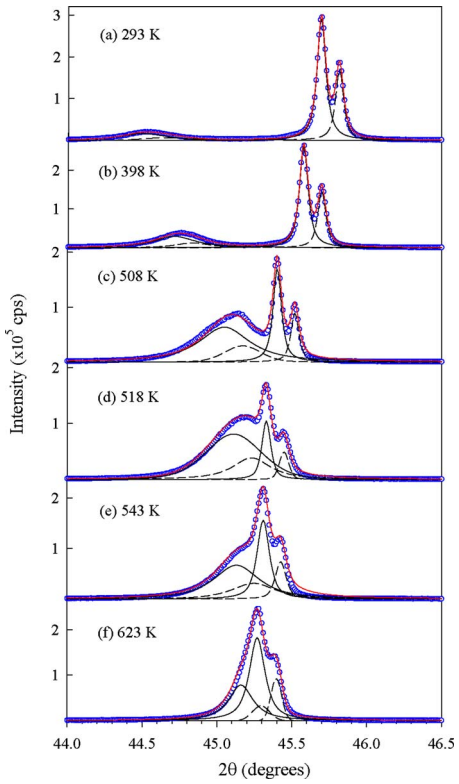

FIG. 3. (Color online) *In situ* temperature-dependent (002) XRD spectra upon ZFH. The solid and dashed lines correlate to the $K\alpha_1$ and $K\alpha_2$ radiations, respectively. The red solid line is the sum of fitting curves.

odomains (or nanotwins). The coexistence of T and T_{NT} phases is confirmed by the (002) XRD as shown in Fig. 3(a), which shows a strong T phase (high-2θ sharp peak) and a minor T_{NT} phase (low-2θ broad peak).

The relation of 2θ-reflection position and d spacing obeys the Bragg law $2d_{hkl}\sin\theta_{hkl}=n\lambda$ for both the $K\alpha_1$ and the $K\alpha_2$ radiations. The d values for the six T domain types are $1/d^2=(h^2+k^2)/a^2+(l^2/c^2)$,[19] where (h,k,l) and (a,b,c) are the domain crystallographic orientation and lattice parameters, respectively. For the (001) cut, the six T domain types have two different d spacings, i.e., $1/d^2=1/a^2$ and $1/d^2=1/c^2$.

At room temperature, as given in Fig. 3(a), the (002) XRD reflection reveals two d spacings, which correspond to the two (001) and four (100) and (010) oriented T domains. Note that (100) and (010) oriented domains have the same d spacing for the T phase. The strong high-2θ sharp peak (T phase) and weak low-2θ broad peak (T_{NT} phase) as shown in Fig. 3(a), indicate that tetragonal nanotwins reside in the FE tetragonal matrix. It is important to know that the nanodomain (or nanotwin) size is much smaller than the coherent length of diffraction radiation. Thus, scattered waves from individual nanodomains coherently superimpose in diffraction and cause broadening of the reflection peaks.[2] The broad diffraction peak can be easily mistaken as monoclinic phases. From the $K\alpha_1$ reflections, the lattice parameters of tetragonal unit cell at room temperature were calculated to be $a_T\cong 3.968$ Å and $c_T\cong 4.069$ Å.

Except for the birefringence color and brightness, as seen in Figs. 2(a) and 2(b), the domain matrix shows no

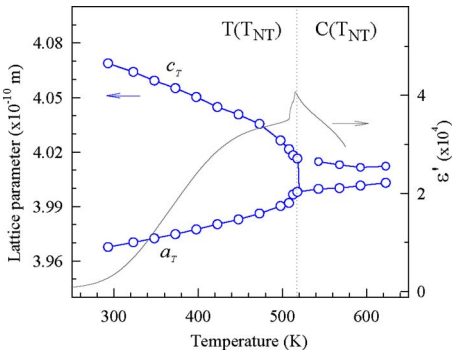

FIG. 4. (Color online) Temperature-dependent lattice parameters obtained upon ZFH. The solid-line background is ε' ($f=50$ kHz) for comparison. The dotted line indicates the Curie temperature $T_C\cong 518$ K.

obvious change in optical extinction angle in the temperature region of 300–460 K, where $\varepsilon'(T)$ exhibits a broad frequency-dependent plateau (or shoulder). The (002) XRD spectra (Fig. 3) and lattice parameters (Fig. 4) do not exhibit any anomaly or discontinuity in the region of 300–460 K. Importantly, as shown in Fig. 3, the relative intensity and fraction of the low-2θ broad peak increase as the temperature increases and reaches a maximum near 518 K, indicating a gradual growth of T-phase nanotwins while the first-order transition is approached upon heating. The appearance of nanotwins can reduce the averaged optical anisotropy and thus decreases the brightness of birefringence in the polarizing microscopy as seen in Fig. 2. In addition, the dynamics of polar nanostructures has been believed to be responsible for the dielectric dispersion in the relaxor FE materials.[21] The strong frequency dispersion observed in ε' (Fig. 1) could be partially associated with nanotwins.

As the temperature increases, as seen in Fig. 2(c), the C phase (with a total optical extinction) begins to appear significantly near 523 K. Note that the dielectric maximum temperature is at $T_m\cong 515$ K as seen in Fig. 1. As given in the inset of Fig. 2(c), the domain matrix goes into a complete total extinction near 525 K, indicating a complete cubic phase. Note that the optimal resolution of the polarizing microscope is about 1 μm due to the diffraction limit. As shown in Fig. 4, the two lattice parameters (a_T and c_T) of the tetragonal unit cell gradually approach each other and then jump to join together at the Curie temperature $T_C\cong 518$ K, indicating a first-order phase transition.

As the temperature increases above $T_C\cong 518$ K, in addition to the C phase (high-2θ narrow peak) a clear low-2θ broad peak was detected as shown in Figs. 3(e) and 3(f). Its relative intensity decreases as temperature increases. The low-2θ broad peak corresponds to T-phase nanotwins (or nanoclusters) which can cause an average C phase and give a total extinction in the polarizing microscopy. Above $T_C\cong 518$ K, the major high-2θ peak corresponds to dipole glass material of C phase and its relative intensity increases as the temperature increases. The existence of T-phase nanotwins above $T_C\cong 518$ K indicates that nanostructure plays an important bridging role to accommodate the spontaneous lattice distortion and minimize the elastic strain energy while a first-order phase transition takes place. Figure 4 gives the

temperature-dependent lattice parameters and dielectric permittivity upon ZFH. Above $T_C \cong 518$ K, the lattice parameter of C phase gradually rises simply due to thermal expansion.

IV. CONCLUSIONS

The unpoled (001)-cut PFN-48%PT crystal demonstrates high frequency-dependent dielectric permittivity and a first-order $T(T_{NT})$-$C(T_{NT})$ phase transition at $T_C \cong 518$ K upon ZFH. Tetragonal nanotwins, which cause broad diffraction peak, remain above $T_C \cong 518$ K and gradually disappear as temperature increases. The nanotwin domains give an average microscopic cubic phase above $T_C \cong 518$ K and exhibit a total extinction in the polarizing microscopy. Nanotwin structures, which often cause broad XRD spectra, were also evidenced apparently in the (001) oriented PMN-30%PT crystal.[22] However, the recent *in situ* temperature-dependent XRD result of the (111)-cut PMN-30%PT crystal did not show obvious imprint of nanotwin structure, implying that the elastic strain energy is smaller in the (111) oriented rhombohedral crystal.[23] Nanotwin structure seems to play an important role in the (001) oriented high-strain FE crystals while phase transition takes place because they can accommodate the spontaneous lattice distortion. The strong dielectric dispersion (Fig. 1) likely correlates with relaxations of mobile charge carrier and nanotwins. This study suggests that the Fe ion is a potential candidate as a *B*-site dopant for enhancing dielectric permittivity.

ACKNOWLEDGMENTS

The authors would like to thank Dr. H. Luo (Shanghai Institute of Ceramics) for the crystals. This work was supported by National Science Council of Taiwan Grant No. 96-2112-M-030-001.

[1] Y. U. Wang, Phys. Rev. B **74**, 104109 (2006).
[2] Y. U. Wang, Phys. Rev. B **76**, 024108 (2007).
[3] H. Wang, J. Zhu, N. Lu, A. A. Bokov, Z. G. Ye, and X. W. Zhang, Appl. Phys. Lett. **89**, 042908 (2006).
[4] Y. Yamashita, Y. Hosono, K. Harada, and N. Yasuda, IEEE Trans. Ultrason. Ferroelectr. Freq. Control **49**, 184 (2002).
[5] J. Chen and R. Panda, Proc.-IEEE Ultrason. Symp., **1**, 235 (2005).
[6] J. Wang, B. Neaton, H. Zheng, V. Nagarajan, S. B. Ogale, B. Liu, D. Viehland, V. Vaithyanathan, D. G. Schlom, U. V. Waghmare, N. A. Spaldin, K. M. Rabe, M. Wuttig, and R. Ramesh, Science **299**, 1719 (2003).
[7] T. Kimura, T. Goto, H. Shintani, K. Ishizaka, T. Arima, and Y. Tokura, Nature (London) **426**, 55 (2003).
[8] G. A. Smolenskii, A. I. Agranovskaia, S. N. Popov, and V. A. Isupov, Sov. Phys. Tech. Phys. **3**, 1981 (1958).
[9] D. N. Astrov, B. I. Al'shin, R. V. Zorin, and L. A. Drobyshev, Sov. Phys. JETP **28**, 1123 (1969).
[10] I. H. Brunskill, H. Schmid, and P. Tissot, Ferroelectrics **37**, 547 (1981).
[11] V. Bonny, M. Bonin, P. Sciau, K. J. Schenk, and G. Chapuis, Solid State Commun. **102**, 347 (1997).
[12] S. A. Ivanov, R. Tellgren, H. Rundlof, N. W. Thomas, and S. Ananta, J. Phys.: Condens. Matter **12**, 2393 (2000).
[13] S. B. Majumder, S. Bhattacharyya, R. S. Katiyar, A. Manivannan, P. Dutta, and M. S. Seehra, J. Appl. Phys. **99**, 024108 (2006).
[14] V. V. S. Sai Sunder and A. M. Umarji, Mater. Res. Bull. **30**, 427 (1995).
[15] X. Meng, K. Z. Baba-Kishi, H. L. Chan, C. L. Choy, and H. Luo, Ferroelectrics **303**, 69 (2004).
[16] J. Wang, X. G. Tang, H. L. W. Chan, C. L. Choy, and H. Luo, Appl. Phys. Lett. **86**, 152907 (2005).
[17] Y. Gao, H. Xu, Y. Wu, T. He, G. Xu, and H. Luo, Jpn. J. Appl. Phys., Part 1 **40**, 4988 (2001).
[18] R. R. Chien, V. H. Schmidt, C.-S. Tu, L.-W. Hung, and H. Luo, Phys. Rev. B **69**, 172101 (2004).
[19] B. D. Cullity, *Elements of X-ray Diffraction*, 2nd ed. (Addison-Wesley, Reading, MA, 1978), pp. 8–10 and p. 501.
[20] G. Xu, H. Hiraka, G. Shirane, and K. Ohwada, Appl. Phys. Lett. **84**, 3975 (2004).
[21] D. Viehland, S. J. Jang, L. E. Cross, and M. Wuttig, Phys. Rev. B **46**, 8003 (1992).
[22] C.-S. Tu, C.-M. Hsieh, R. R. Chien, V. H. Schmidt, F.-T. Wang, and W. S. Chang, J. Appl. Phys. **103**, 074117 (2008).
[23] C.-S. Tu, H.-T. Chuang, S.-C. Lee, R. R. Chien, V. H. Schmidt, and H. Luo, J. Appl. Phys. **104**, 024110 (2008).